Published in final edited form as:
Dent Mater. 2012 May ; 28(5): 573–583. doi:10.1016/j.dental.2012.01.006.

Antibacterial and physical properties of calcium-phosphate and calcium-fluoride nanocomposites with chlorhexidine

Lei Cheng[1,2], **Michael D. Weir**[1], **Hockin H. K. Xu**[1,3,4,5], **Alison M. Kraigsley**[6], **Nancy J. Lin**[6], **Sheng Lin-Gibson**[6], and **Xuedong Zhou**[2]

[1]Biomaterials & Tissue Engineering Division, Dept. of Endodontics, Prosthodontics and Operative Dentistry, University of Maryland Dental School, Baltimore, MD 21201, USA

[2]State Key Laboratory of Oral Diseases, West China College of Stomatology, Sichuan University, Chengdu, China

[3]Center for Stem Cell Biology & Regenerative Medicine, University of Maryland School of Medicine, Baltimore, MD 21201, USA

[4]University of Maryland Marlene and Stewart Greenebaum Cancer Center, University of Maryland School of Medicine, Baltimore, MD 21201, USA

[5]Department of Mechanical Engineering, University of Maryland, Baltimore County, MD 21250

[6]Biomaterials Group, Polymers Division, National Institute of Standards & Technology, Gaithersburg, MD 20899, USA

Abstract

Objectives—Previous studies have developed calcium phosphate and fluoride releasing composites. Other studies have incorporated chlorhexidine (CHX) particles into dental composites. However, CHX has not been incorporated in calcium phosphate and fluoride composites. The objectives of this study were to develop nanocomposites containing amorphous calcium phosphate (ACP) or calcium fluoride (CaF_2) nanoparticles and CHX particles, and investigate *S. mutans* biofilm formation and lactic acid production for the first time.

Methods—Chlorhexidine was frozen via liquid nitrogen and ground to obtain a particle size of 0.62 μm. Four nanocomposites were fabricated with fillers of: Nano ACP; nano ACP+10% CHX; nano CaF_2; nano CaF_2+10% CHX. Three commercial materials were tested as controls: A resin-modified glass ionomer, and two composites. *S. mutans* live/dead assay, colony-forming unit (CFU) counts, biofilm metabolic activity, and lactic acid were measured.

Correspondence: Dr. Hockin H. K. Xu, Professor, Director of Biomaterials & Tissue Engineering Division, Department of Endodontics, University of Maryland Dental School, Baltimore, MD 21201, (hxu@umaryland.edu), and Dr. Xuedong Zhou, Professor, Dean, West China College of Stomatology, Sichuan University, China (zhouxd@scu.edu.cn).

Results—Adding CHX fillers to ACP and CaF_2 nanocomposites greatly increased their antimicrobial capability. ACP and CaF_2 nanocomposites with CHX that were inoculated with *S. mutans* had a growth medium pH > 6.5 after 3 d, while the control commercial composites had a cariogenic pH of 4.2. Nanocomposites with CHX reduced the biofilm metabolic activity by 10–20 folds and reduced the acid production, compared to the controls. CFU on nanocomposites with CHX were three orders of magnitude less than that on commercial composite. Mechanical properties of nanocomposites with CHX matched a commercial composite without fluoride.

Significance—The novel calcium phosphate and fluoride nanocomposites could be rendered antibacterial with CHX to greatly reduce biofilm formation, acid production, CFU and metabolic activity. The antimicrobial and remineralizing nanocomposites with good mechanical properties may be promising for a wide range of tooth restorations with anti-caries capabilities.

Keywords

dental nanocomposite; calcium phosphate; calcium fluoride; chlorhexidine; stress-bearing; *S. mutans* biofilm; caries inhibition

1. Introduction

Nearly 200 million dental restorations are placed annually in the USA [1]. Resin composites are increasingly used for dental caries restorations because of their esthetics and direct-filling capability [2–8]. Remarkable progress has led to esthetic composite restoratives with less removal of tooth structures, enhanced load-bearing properties, and improved clinical performance [9–15]. However, secondary caries at the restoration margins is identified as a main limitation to the longevity of the restorations [16–18]. The replacement of existing restorations accounts for 50% to 70% of all restorations performed [19,20]. Replacement dentistry costs $5 billion annually in the U. S. alone [21]. Dental caries is a dietary carbohydrate-modified bacterial infectious disease, and is one of the most common bacterial infections in humans [22–24]. The basic mechanism of caries is demineralization of dental tissue (enamel/dentin) via acid generated by bacterial biofilms (dental plaque) [25–27]. Acidogenic bacterial growth and biofilm formation in the presence of fermentable carbohydrates are known to be responsible for caries. However, resin composites do not hinder bacteria colonization and plaque formation. On the contrary, previous studies have shown that composites allow more accumulation of plaque on their surfaces than other restoratives [28–30].

Efforts are underway to develop novel antibacterial composites to reduce caries. One approach involves the incorporation of antibacterial monomers to decrease the viability of bacteria such as *Streptococcus mutans* (*S. mutans*) [4,29,31]. In one study, a polymerizable bactericidal monomer, 12-methacryloyloxydodecylpyridinium bromide (MDPB), was immobilized in the resin which reduced bacteria growth via contact inhibition [4]. In another, ionic liquid dimethacrylate monomers that contained quaternary ammoniums groups were used to develop antimicrobial resins, which reduced bacterial colonization [32]. Other studies incorporated chlorhexidine (CHX) particles as fillers into dental resin composites, which resulted in CHX release and reduced bacteria growth [33–35]. CHX particles were also mixed into glass ionomer cements [36], thus combining antimicrobial activity with fluoride ions (F) [37].

Another promising class of composites consists of resins filled with calcium phosphate (CaP) particles of about 1 μm to 55 μm in sizes [38–40]. These composites released supersaturating levels of calcium (Ca) and phosphate (PO_4) ions and remineralized tooth lesions *in vitro* [39,40]. Recently, CaP nanoparticles of about 100 nm in size were

synthesized via a spray-drying technique for the first time [41,42]. Composites containing CaP nanoparticles with high specific surface areas were found to release high levels of Ca and PO_4 while possessing mechanical properties nearly two-fold those of previous CaP composites [41,42]. Nanocomposites containing CaF_2 nanoparticles were also developed that released fluoride (F) ions matching that of a resin-modified glass ionomer [43,44]. The mechanical properties of the CaF_2 nanocomposite were much higher than that of resin-modified glass ionomer, and matched those of commercial composites with little F release [43,44]. However, there has been no report of CaP and CaF_2 nanocomposites containing CHX to achieve the triple benefits of remineralization, antibacterial, and load-bearing capabilities.

Therefore, the objectives of this study were to combine CHX with CaP or CaF_2 nanoparticles into the nanocomposites, and to determine the mechanical and antibacterial properties. It was hypothesized that: (1) incorporating CHX into CaP and CaF_2 nanocomposites will impart a potent antibacterial capability to diminish *S. mutans* biofilm viability and therefore reduce the acid production; and (2) the mechanical properties of the CaP and CaF_2 nanocomposites containing CHX will match those of commercial composites that have no ion release or antibacterial capability.

2. Materials and methods

2.1. Fabrication of CaP and CaF_2 nanocomposites containing CHX

Nanoparticles of amorphous calcium phosphate (ACP), $Ca_3(PO_4)_2$, were synthesized via a spray-drying technique [45]. ACP is an important compound because it is a precursor that can convert to apatite, similar to the minerals in tooth enamel and dentin. A spraying solution was prepared by dissolving calcium carbonate ($CaCO_3$, Fisher, Fair Lawn, NJ) and dicalcium phosphate anhydrous ($CaHPO_4$) (J. T. Baker, Phillipsburg, NJ) into an acetic acid solution. This solution was sprayed through a nozzle into a heated chamber [46]. The water and volatile acid were evaporated and expelled into an exhaust-hood. The dried particles were collected by an electrostatic precipitator [45]. Transmission electron microscopy (TEM, 3010-HREM, JEOL, Peabody, MA) was used to examine the ACP particles.

CaF_2 nanoparticles were synthesized using the same spray-drying apparatus, except that a two-liquid nozzle was employed [43,47]. This allowed two solutions to be mixed during atomization: $Ca(OH)_2$ and NH_4F. The two solutions were atomized leading to the formation of CaF_2 nanoparticles: $Ca(OH)_2 + NH_4F \rightarrow CaF_2 + NH_4OH$. The NH_4OH was removed as NH_3 and H_2O vapors. TEM was used to examine the CaF_2 particles.

Chlorhexidine diacetate (Sigma, St. Louis, MO) was frozen via liquid nitrogen, and then ground in a mortar and pestle to obtain a fine particle size. The particles were sputter coated with gold and examined in a scanning electron microscope (SEM, FEI Quanta 200, Hillsboro, OR). These particles are referred to as CHX. The sizes of 100 random CHX particles were measured via SEM in this study.

Barium aluminosilicate glass particles with a mean diameter of 1.4 μm (Caulk/Dentsply, Milford, DE) were used as a co-filler and silanized with 4% (all mass fractions) 3-methacryloxypropyltrimethoxysilane and 2% n-propylamine. For ACP nanocomposite, a resin of Bis-GMA (bisphenol glycidyl dimethacrylate) and TEGDMA (triethylene glycol dimethacrylate) at 1:1 ratio was rendered light-curable with 0.2% camphorquinone and 0.8% ethyl 4-N,N-dimethylaminobenzoate [45]. For the CaF_2 nanocomposite, because the paste was relatively opaque, a two-part chemically-activated resin was used. The initiator resin consisted of 48.975% Bis-GMA, 48.975% TEGDMA, 0.05% 2,6-di-*tert*-butyl-4-

methylphenol, and 2% benzoyl-peroxide. The accelerator resin consisted of 49.5% Bis-GMA, 49.5% TEGDMA, and 1.0% *N*,*N*-dihydroxyethyl-*p*-toluidine [44].

Four nanocomposites were made with the following filler mass fractions: (1) 30% nano ACP + 35% glass (referred to as "NanoACP"); (2) 30% nano ACP + 25% glass + 10% CHX (referred to as "NanoACP+CHX"); (3) 30% nano CaF_2 + 35% glass ("NanoCaF_2"); (4) 30% nano CaF_2 + 25% glass + 10% CHX ("NanoCaF_2+CHX").

The glass and nanoparticle filler levels were selected following previous studies [44,48]. The CHX filler level was based on previous studies which ranged from 0.5% to 33% [33–36]. The total filler mass fraction of 65% yielded a cohesive paste. The paste was placed into rectangular molds of (2 × 2 × 25) mm for mechanical testing, and disk molds of 9 mm in diameter and 2 mm in thickness for biofilm experiments. NanoCaF_2 specimens were self-cured. NanoACP specimens were photo-cured (Triad 2000, Dentsply, York, PA) for 1 min on each side.

Three commercial materials were tested as controls. A resin-modified glass ionomer (Vitremer, 3M, St. Paul, MN), referred to as "RMGI", consisted of fluoroaluminosilicate glass, and a light-sensitive, aqueous polyalkenoic acid. Indications include Class III, V and root-caries restoration, Class I and II in primary teeth, and core-buildup. A powder/liquid mass ratio of 2.5/1 was used according to the manufacturer. A composite with nanofillers of 40–200 nm and a low level of F release was used (Heliomolar, Ivoclar, Amherst, NY), and is referred to as "CompositeF". The fillers were silica and ytterbium-trifluoride with a filler level of 66.7%. Heliomolar is indicated for Class I, II, III, IV and V restorations. Renamel (Cosmedent, Chicago, IL) served as a non-releasing control, and is referred to as "CompositeNoF". It consisted of nanofillers of 20–40 nm with 60% fillers in a multifunctional methacrylate ester resin [49]. Renamel is indicated for Class III, IV, and V restorations. Specimens were photo-cured in the same manner as the ACP nanocomposite.

2.2. Flexural testing

Flexural strength and elastic modulus were measured using a three-point flexural test with a 10 mm span at a crosshead-speed of 1 mm/min on a computer-controlled Universal Testing Machine (5500R, MTS, Cary, NC). Flexural strength (S) was calculated by: $S = 3P_{max}L/(2bh^2)$, where P_{max} is the fracture load, L is span, b is specimen width and h is specimen thickness. Elastic modulus (E) was calculated by: $E = (P/d)(L^3/[4bh^3])$, where load P divided by displacement d is the slope of the load-displacement curve in the linear elastic region.

2.3. CHX release measurement

CHX release was measured for NanoACP+CHX and NanoCaF_2+CHX composites. A physiological-like buffer solution with pH of 7 (133 mM NaCl, 50 mM 4-(2-hydroxyethyl)-1-piperazineethanesulfonic acid, HEPES) was prepared. Following previous studies [41–44], three specimens of (2 × 2 × 12) mm were immersed in 50 mL solution. The CHX concentrations were measured at days 1, 2, 3, 7, 14, 21, and 28. At each time period, aliquots of 200 μL were removed and replaced by fresh solution. A series of CHX reference solutions was prepared and a standard curve was constructed. The absorbance at 255 nm was measured via a microplate reader (SpectraMax M5, Molecular Devices, Sunnyvale, CA).

2.4. *S. mutans* inoculation and pH measurement

The use of *S. mutans* (ATCC 700610, UA159, American Type Culture, Manassas, VA) was approved by the University of Maryland. *S. mutans* is a cariogenic, aerotolerant anaerobic bacterium and the primary causative agent of dental caries [22]. Brain heart infusion (BHI)

broth (BD, Franklin Lakes, NJ) supplemented with 0.2% sucrose is termed “growth medium”. Fifteen μL of stock bacteria was added into 15 mL of growth medium and incubated at 37 °C with 5% CO_2 for 16 h. During this culture, the *S. mutans* were suspended in the BHI broth. Then, this *S. mutans* culture was diluted 10-fold in growth medium to form the inoculation medium [50].

The composite disks were sterilized with ethylene oxide (Anprolene AN 74i, Andersen, Haw River, NC). Each disk was placed in a well of a 24-well plate, and 1.5 mL of the inoculation medium was added to each well. The samples were incubated at 5% CO_2 and 37 °C for 24 h to form the initial biofilms on the disk. At 24 h, each disk with biofilm was transferred to a new 24-well plate containing 1.5 mL of fresh growth medium. The pH of the medium was measured via a pH meter (Accumet Excel XL25, Fisher, Pittsburgh, PA) from 24 h to 48 h. pH measurements were not collected during the first 24 h of culture, because the non-adherent bacteria in the growth medium could contribute to the pH changes. In this way, the measured pH was solely related to the biofilm on the composite, and there was no contribution from planktonic bacteria in the media. At 48 h, each disk was transferred to a new 24-well plate containing 1.5 mL of fresh growth medium. The pH of the medium was measured again from 48 h to 72 h.

2.5. Live/dead assay

Each disk was placed in a well of a 24-well plate, inoculated with 1.5 mL of inoculation medium, and cultured for 1 d (initial biofilm), or 3 d (mature biofilm). The growth medium was changed every 24 h, by transferring the disks to a new 24-well plate with fresh growth medium. After 1 d or 3 d, the biofilms on the disks were stained using the BacLight live/dead bacterial viability kit (Molecular Probes, Eugene, OR). Live bacteria were stained with Syto 9 to produce green fluorescence, and bacteria with compromised membranes were stained with propidium iodide to produce red fluorescence. The stained disks were imaged using laser scanning confocal microscopy (TCS SP5, Leica, Germany). A minimum of three x–y images were collected at random locations on each disk. At each time point, a minimum of three disks were evaluated for each material yielding a minimum of 9 images for each sample.

2.6. Lactic acid production and viable cell counts

After 3 d, mature biofilms were formed on the disks. Each disk was rinsed in cysteine peptone water (CPW) to remove loose bacteria, and placed in a new 24-well plate. Then, 1.5 mL of buffered peptone water (BPW) supplemented with 0.2% sucrose was added to each well. The reason for using the BPW media was that the mature biofilm would remain stable during this 3 h culture for the acid production assay. In addition, BPW has a relatively high buffer capacity, so the pH should not become significantly acidic, as a low pH could hinder bacterial acid production. The samples were incubated at 5% CO_2 and 37 °C for 3 h to allow the biofilms to produce acid. After 3 h, the BPW solutions were stored for lactate analysis. Lactate concentrations in the BPW solutions were determined using an enzymatic (lactate dehydrogenase) method [51]. The microplate reader was used to measure the absorbance at 340 nm (optical density OD_{340}) for the collected BPW solutions. Standard curves were prepared using a standard lactic acid (Supelco Analytical, Bellefonte, PA).

After treatment for lactic acid production, colony-forming unit (CFU) counts were used to quantify the total number of viable bacteria present on each disk. When biofilms are properly dispersed and diluted, each viable bacterium results in a single, countable colony on an agar plate. The disks were transferred into tubes with 2 mL CPW. The biofilms were harvested by sonication (3510R-MTH, Branson, Danbury, CT) for 3 minutes, and then vortexing at maximum speed for 20 s using a vortex mixer (Fisher, Pittsburgh, PA), thus

removing and dispersing the biofilms from the sample disks. The bacterial suspensions were serially diluted, spread onto BHI agar plates, and incubated for 3 d at 5% CO_2 and 37 °C. The number of colonies that grew were counted and used, along with the dilution factor, to calculate total CFUs on each composite disk.

2.7. MTT metabolic assay

Disks were placed in a 24-well plate, inoculated with 1.5 mL of the inoculation medium, and cultured for 1 d or 3 d. Each disk was then transferred to a new 24-well plate for the MTT (3-(4,5-Dimethylthiazol-2-yl)-2,5-diphenyltetrazolium bromide) assay, a colorimetric assay that measures the enzymatic reduction of MTT, a yellow tetrazole, to formazan [52]. One mL of MTT dye (0.5 mg/mL MTT in PBS) was added to each well and incubated at 37 °C in 5% CO_2 for 1 h. During this process, metabolically active bacteria metabolized the MTT and reduced it to purple formazan inside the living cells. After 1 h, the disks were transferred to a new 24-well plate, 1 mL of dimethyl sulfoxide (DMSO) was added to solubilize the formazan crystals, and the plate was incubated for 20 min with gentle mixing at room temperature in the dark. After brief mixing via pipetting, 200 μL of the DMSO solution from each well was transferred to a 96-well plate, and the absorbance at 540 nm (OD_{540}) was measured via the microplate reader. A higher absorbance indicates a higher formazan concentration, which in turn indicates more metabolic activity in the biofilm present on the composite disk.

One-way and two-way analyses of variance (ANOVA) were performed to detect the significant effects of the variables. Tukey's multiple comparison test was used to compare the data at a p-value of 0.05. Each standard deviation (sd) serves as the estimate for the standard uncertainty associated with a particular measurement.

3. Results

Fig. 1A plots the histogram of CHX particle size distribution. Based on 100 particles measured via SEM, the particle size ranged from approximately 0.1 μm to 5 μm, with (mean ± sd; n = 100) of (0.62 ± 0.48) μm. The CHX release from the ACP nanocomposite and CaF_2 nanocomposite is plotted in (B) (mean ± sd; n = 3). The CHX release from the ACP nanocomposite was similar to that of the CaF_2 nanocomposite ($p > 0.1$).

Fig. 2 shows TEM images of nanoparticles and composite mechanical properties: (A) Example of smaller ACP nanoparticles, (B) example of ACP clusters, (C) CaF_2 nanoparticles, (D) flexural strength and (E) elastic modulus after 1 d and 28 d of immersion. In (A), arrows indicate individual ACP particles that overlapped a larger ACP particle. In (B), arrows indicate individual ACP particles near a cluster. The cluster appeared to contain numerous small particles, which likely had stuck to form the cluster in the spray-drying chamber before they were completely dried. In general, the individual ACP particles had sizes of the order of 10 nm, and the clusters had sizes of about 100–300 nm. Measurement of 100 random particles yielded an average size of 37 nm for the individual ACP particles, and an average size of 225 nm for the ACP clusters. Similar features were observed for CaF_2 in (C), and measurement of 100 random particles yielded an average size of 20 nm for the individual CaF_2 particles, and an average size of 306 nm for CaF_2 clusters.

In Fig. 2D, CompositeNoF, NanoACP, NanoCaF_2, and NanoCaF_2+CHX had a significant decrease in strength from 1 d to 28 d ($p < 0.05$). CompositeF, CompositeNoF, NanoACP, and NanoCaF_2 had strengths similar to each other at 28 d ($p > 0.1$). The strengths of NanoACP+CHX and NanoCaF_2+CHX at 28 d were 2-fold that of RMGI ($p < 0.05$). In 2E, elastic moduli in general were similar to each other for the different materials at 1 d and 28 d.

The pH of biofilm medium is plotted in Fig. 3. (A) pH measurements were started at 24 h, when the medium was changed, and then collected hourly. (B) Then the pH was measured again after the medium change at 48 h. In (A), for NanoCaF$_2$+CHX and NanoACP+CHX, the pH remained at 6.5 or higher. For all other materials, the pH decreased with time, reaching 4.7 for RMGI, 4.6 for NanoCaF$_2$, and 4.2 for the other composites at 48 h. Comparing (A) with (B) shows a similar trend and similar end pH values, indicating that the effect of inhibiting bacteria growth and acid production for the CHX composites was maintained over 3 d.

Images of biofilms stained with the live/dead stain are shown in Fig. 4. The live bacteria appear green, and the compromised bacteria appear red. In some areas, the live and compromised (likely dead) bacteria are closely associated and/or colocalized, hence the red color was mingled with green to yield the yellow and orange colors. At 1 d, the biofilms were predominantly viable in (A) and (C), whereas in (B), biofilm surface coverage was slightly patchy and there was some cell death. In (D), the biofilms grown on the NanoACP +CHX also had patchy surface coverage and had increased numbers of dead bacteria relative to (A) to (C). The biofilm structure and viability for NanoCaF$_2$+CHX at 1 d (not shown) had similar features to those in (D), with even more cell death evident by more yellow in the images.

At 3 d, *S. mutans* had formed a mature biofilm in Fig. 4E to 4G, where the bacteria were primarily alive, with RMGI having slightly more dead bacteria. Biofilms on CompositeNoF and NanoCaF$_2$ (not shown) were similar to those in (E) and (G). NanoACP+CHX in (H) had significantly more dead bacteria. NanoCaF$_2$+CHX had similar images to (H), with increased cell death evident by mostly yellow and red staining and very little green present.

Fig. 5 plots results on (A) lactic acid production, and (B) CFU counts. Biofilm on CompositeNoF produced the most acid, closely followed by that of nano ACP. Between F-releasing materials, biofilm on CompositeF had the most acid, while biofilms on NanoCaF$_2$ and RMGI had similarly lower acid production. Acid production on composites with CHX was nearly 10-fold less than that on CompositeNoF. In (B), the CFU counts were $\approx 10^9$ per disk for CompositeNoF, and $\approx 10^8$ for all other materials without CHX. CFU counts for nanocomposites with CHX were reduced 1,000-fold (to $\approx 10^6$) from those of CompositeNoF.

The MTT results are plotted in Fig. 6 for (A) 1 d, and (B) 3 d. In each plot, values (mean ± sd; n = 6) with dissimilar letters are significantly different ($p < 0.05$). In (A), CompositeNoF had the highest absorbance. The two nanocomposites containing CHX had absorbance 10-fold less than that of RMGI, and 20-fold less than that of CompositeNoF. A similar trend was maintained at 3 d in (B), although the absorbance was 1.5 to 2 fold higher than that at 1 d.

4. Discussion

The present study investigated the effects of novel nanocomposites containing ACP or CaF$_2$ nanoparticles and CHX on biofilm formation, viability, acid production, and metabolic activity for the first time. An important approach to the inhibition of demineralization and the promotion of remineralization was the development of CaP composites [38–41]. Previous studies showed that the remineralization of tooth lesions was greatly promoted by increasing the solution calcium and phosphate ion concentrations [39,40]. Composites containing CaP particles released Ca and PO$_4$ ions to supersaturating levels with respect to tooth mineral, and were shown to protect the teeth from demineralization, and even regenerate lost tooth mineral *in vitro* [39,40]. A recent study showed that the new nano ACP

composite released Ca and PO_4 ions at concentrations matching those of traditional CaP composites known to remineralize tooth lesions, while having much higher mechanical properties [45]. Another study demonstrated that the new nano CaF_2 composite released F ions at similar amounts to a commercial resin-modified glass ionomer, while having mechanical properties equivalent to a commercial composite without F release [44]. Previous studies indicated that the release of Ca, PO_4 and F ions could lead to the remineralization of the tooth structure [24,25,39,40,53]. In the present study, the composites not only could release Ca, PO_4 and F ions [43–45], but also increased the pH (Fig. 3) which could have an additional effect on the remineralization of the tooth structure. Further studies are needed to measure the mineral contents of tooth structures with the use of the antibacterial composites containing ACP and CaF_2 nanoparticles.

CHX particles have been incorporated into glass ionomer materials [36,37] and dental polymeric composites to render the filling materials antibacterial [33,35]. The present study showed that the CHX release was relatively high in the first week and then plateaued after 2 weeks, which is similar to previous studies [36]. The percentage of CHX released from the ACP and CaF_2 nanocomposites during one month of immersion was relatively small (about 2%), which is comparable to previous studies. Such a small amount of CHX release, while having an antibacterial effect near the surface of the tooth cavity restoration locally, is expected to have a negligible systemic effect. In previous studies, the CHX released from a glass ionomer cement was about 3–5% after 240 d [36]. Another study showed that the percentage of CHX released from a dental composite was about 10% after 4 months of immersion in a pH 6 solution; when the solution pH was reduced to 4, the CHX release increased to 50% in 4 months due to polymer degradation [35]. The present study showed that even a small amount of the CHX release from the nanocomposites greatly reduced acidogenic bacterial CFU counts, biofilm viability, biofilm formation, biofilm metabolic activity, and therefore lactic acid production. The 2% release indicates a large reservoir of CHX remaining in the composite. A previous study estimated that if the CHX reservoir in the resin was fully utilized, the release could last 6–10 years [35].

Most previous studies [33,34,36,37] did not mention attempts to obtain fine CHX particles by grinding the as-received particles, which were about 40 μm in diameter for the CHX diacetate from Sigma. A particle size of 40 μm is much larger than the glass fillers in dental composites, which are typically about 1 μm or less. One study reported the grinding of the as-received CHX, yielding a particle size of 13.5 μm [35]. Preliminary studies failed to obtain smaller CHX particles, until the use of liquid nitrogen to chill the CHX prior to grinding. The lower temperature appeared to embrittle and help shatter the particles, yielding an average particle size of 0.62 μm in the present study. A small CHX particle size could improve the polishability and mechanical properties of the composite. Previous studies on CHX composites did not report their mechanical properties [33,35]. In the present study, after 28 d immersion, the strength for NanoACP+CHX was approximately 80% that without CHX. A similar 20% strength loss occurred for NanoCaF_2. However, the strength of the nanocomposites containing CHX was only slightly lower than the commercial composite without CHX. The strength of the nanocomposites containing CHX was twice that of a commercial resin-modified glass ionomer.

Previous studies have shown that bacteria will colonize surfaces and form biofilms, which are heterogeneous structures consisting of cell clusters embedded in an extracellular matrix [54]. Acidogenic bacteria in dental plaque, such as *S. mutans*, metabolize carbohydrates to acids and can result in a local plaque pH drop to 4.5 or 4 after a sucrose rinse. Acids cause demineralization of the tooth structure beneath the biofilm. Studies have shown that there is a critical pH of about 5.5, below which demineralization dominates, leading to a net enamel mineral dissolution [55]. Therefore, it would be highly desirable for the local pH at the tooth

surface to remain greater than 5.5 in order to inhibit secondary caries at the restoration-tooth interface. The NanoACP+CHX and NanoCaF$_2$+CHX likely slowed down or eliminated the bacterial growth, reducing the acid production by the bacteria, thereby yielding a pH of 6.5 or higher. In contrast, the two commercial composites had pH below 4.5. It should be noted that although the biofilms likely had a dominant effect on the pH of the media, the materials such as the resin-modified glass ionomer and the NanoACP composite could also affect the pH in the absence of a biofilm [48]. Hence, the measured pH resulted from contributions from the material and the biofilm. The results of this study demonstrated that NanoACP +CHX and NanoCaF$_2$+CHX composites with *S. mutans* biofilms in the presence of sucrose were able to maintain the pH at a safe level to inhibit tooth mineral dissolution.

Another potential benefit of nanocomposites containing CHX is the ability to reduce biofilm acid production, resulting in a near neutral pH. The biofilm surrounding a tooth caries likely has a low pH, and may therefore have a high proportion of acidogenic, aciduric (acid-tolerant) bacteria and a low proportion of other benign bacteria that are less acid-tolerant [22,56]. Restorations that release CHX can potentially kill all the bacteria in the vicinity. Eventually, the CHX release will be exhausted, and new biofilms will form. Because the pH has been close to neutral during the CHX release, the new biofilm could have a less pathogenic composition as compared to the acidogenic biofilm that likely would have regrown, had there been no CHX treatment. Indeed, without the CHX release, the repeated acidification in the plaque would likely have continued, resulting in even more predominance of acidogenic and aciduric bacteria such as *S. mutans* [23]. Compared to the commercial composites that had a pH of 4.2 in the biofilm medium, the pH in the biofilm medium of the new CHX-releasing nanocomposites was greater than 6.5. Thus, these new composites may be able to promote recolonization of the area with benign bacteria and a normal oral flora (with < 1% acidogenic bacteria [25]). This effect may help prevent the dominance of cariogenic bacteria and hence help inhibit dental caries.

It is interesting to note that the NanoCaF$_2$+CHX had a higher pH than that of NanoACP +CHX. The mechanism for this is likely that the F ion release helped reduce the acid production of the bacteria, via the inhibition of metabolic pathways such as the fermentation pathway for lactic acid production [54]. A previous study used a constant depth film fermentor (CDFF) model and showed that while F treatment had little effect on *S. mutans* viability, it did reduce the acid production of the bacteria [53]. This notion is also supported by the higher pH of RMGI and NanoCaF$_2$ than the pH of CompositeNoF. These results are corroborated by the F-containing materials having lower lactic acid production and CFU, than the commercial CompositeNoF. Therefore, the following two points should be noted: (1) While the release of Ca and PO_4 ions are beneficial in remineralization, the incorporation of CHX was needed in NanoACP to maintain a safe (non-demineralizing) pH of 6.5; (2) the additional F release of NanoCaF$_2$+CHX was beneficial in further reducing the lactic acid production of bacteria.

Compared to the CompositeNoF, the biofilm acid production on NanoACP+CHX and NanoCaF$_2$+CHX was reduced by 10 fold. The metabolic activity, related to the bacteria metabolism, was reduced by 10 to 20 fold. The flexural strength and elastic modulus of the nanocomposites with CHX were not significantly different from those of CompositeNoF after 28 d of immersion. According to the manufacturer, CompositeNoF (Renamel) is indicated for Class III, IV, and V restorations. This suggests that the new nanocomposites containing fine CHX particles may also be suitable for these applications. Further study is needed to improve and optimize the ACP and CaF$_2$ nanocomposites, and to systematically investigate their mechanical and physical properties as well as anti-caries capabilities.

5. Conclusion

The present study developed novel nanocomposites containing ACP and CaF_2 nanoparticles and CHX particles and determined their effects on *S. mutans* biofilm formation, acid production, CFU, and metabolic activity for the first time. Incorporating CHX into the ACP and CaF_2 nanocomposites imparted a potent antibacterial capability. The *S. mutans* biofilm-coated ACP and CaF_2 nanocomposites containing CHX maintained a growth medium pH at a safe level of above 6.5, while that of commercial composites had a cariogenic pH of 4.2, a level known to cause tooth lesions. The new nanocomposites reduced the biofilm acid production and metabolic activity by 10–20 times, compared to a commercial composite. Mechanical properties of the new nanocomposites matched those of a commercial composite without fluoride. These novel ACP and CaF_2 nanocomposites have the mechanical properties to be used in restorations where the commercial control composites are used, and could potentially inhibit biofilm formation, lactic acid production and caries. Further studies are needed to optimize the nanocomposites and investigate the anti-caries capabilities.

Acknowledgments

We thank Dr. L. C. Chow and Dr. S. Takagi of the Paffenbarger Research Center of the American Dental Association Foundation and Dr. J. M. Antonucci of the National Institute of Standards and Technology (NIST) for discussions, and Dr. Qianming Chen at the West China College of Stomatology for help. We are very grateful to Esstech (Essington, PA) and Ivoclar Vivadent (Amherst, NY) for donating the materials. This study was supported by NIH R01 grants DE17974 and DE14190 (HX), NIDCR-NIST Interagency Agreement Y1-DE-7005-01, University of Maryland Dental School, NIST, and West China College of Stomatology.

References

1. American Dental Association (ADA). The 1999 survey of dental services rendered. Chicago, IL: ADA Survey Center; 2002.
2. Ferracane JL. Current trends in dental composites. Crit Rev Oral Biol Med. 1995; 6:302–318. [PubMed: 8664421]
3. Bayne SC, Thompson JY, Swift EJ, Stamatiades P, Wilkerson M. A characterization of first-generation flowable composites. J Am Dent Assoc. 1998; 129:567–577. [PubMed: 9601169]
4. Imazato S. Review: Antibacterial properties of resin composites and dentin bonding systems. Dent Mater. 2003; 19:449–457. [PubMed: 12837391]
5. Xu X, Ling L, Wang R, Burgess JO. Formation and characterization of a novel fluoride-releasing dental composite. Dent Mater. 2006; 22:1014–1023. [PubMed: 16378636]
6. Krämer N, García-Godoy F, Reinelt C, Frankenberger R. Clinical performance of posterior compomer restorations over 4 years. Am J Dent. 2006; 19:61–66. [PubMed: 16555660]
7. Wan Q, Sheffield J, McCool J, Baran GR. Light-curable dental composites designed with colloidal crystal reinforcement. Dent Mater. 2008; 24:1694–1701. [PubMed: 18499245]
8. Drummond JL. Degradation, fatigue, and failure of resin dental composite materials. J Dent Res. 2008; 87:710–719. [PubMed: 18650540]
9. Lim BS, Ferracane JL, Sakaguchi RL, Condon JR. Reduction of polymerization contraction stress for dental composites by two-step light-activation. Dent Mater. 2002; 18:436–444. [PubMed: 12098572]
10. Ruddell DE, Maloney MM, Thompson JY. Effect of novel filler particles on the mechanical and wear properties of dental composites. Dent Mater. 2002; 18:72–80. [PubMed: 11740967]
11. Drummond JL, Bapna MS. Static and cyclic loading of fiber-reinforced dental resin. Dent Mater. 2003; 19:226–231. [PubMed: 12628435]
12. Lu H, Stansbury JW, Bowman CN. Impact of curing protocol on conversion and shrinkage stress. J Dent Res. 2005; 84:822–826. [PubMed: 16109991]
13. Ferracane JL. Hygroscopic and hydrolytic effects in dental polymer networks. Dent Mater. 2006; 22:211–222. [PubMed: 16087225]

14. Watts DC, Issa M, Ibrahim A, Wakiaga J, Al-Samadani K, Al-Azraqi M, et al. Edge strength of resin-composite margins. Dent Mater. 2008; 24:129–133. [PubMed: 17580089]
15. Samuel SP, Li S, Mukherjee I, Guo Y, Patel AC, Baran GR, Wei Y. Mechanical properties of experimental dental composites containing a combination of mesoporous and nonporous spherical silica as fillers. Dent Mater. 2009; 25:296–301. [PubMed: 18804855]
16. Mjör IA, Moorhead JE, Dahl JE. Reasons for replacement of restorations in permanent teeth in general dental practice. International Dent J. 2000; 50:361–366.
17. Sarrett DC. Clinical challenges and the relevance of materials testing for posterior composite restorations. Dent Mater. 2005; 21:9–20. [PubMed: 15680997]
18. Sakaguchi RL. Review of the current status and challenges for dental posterior restorative composites: clinical, chemistry, and physical behavior considerations. Dent Mater. 2005; 21:3–6. [PubMed: 15680996]
19. Deligeorgi V, Mjor IA, Wilson NH. An overview of reasons for the placement and replacement of restorations. Prim Dent Care. 2001; 8:5–11. [PubMed: 11405031]
20. Frost PM. An audit on the placement and replacement of restorations in a general dental practice. Prim Dent Care. 2002; 9:31–36. [PubMed: 11901789]
21. Jokstad A, Bayne S, Blunck U, Tyas M, Wilson N. Quality of dental restorations. FDI Commision Projects 2–95. International Dent J. 2001; 51:117–158.
22. Loesche WJ. Role of *Streptococcus mutans* in human dental decay. Microbiological Reviews. 1986; 50:353–380. [PubMed: 3540569]
23. van Houte J. Role of micro-organisms in caries etiology. J Dent Res. 1994; 73:672–681. [PubMed: 8163737]
24. Featherstone JD. The science and practice of caries prevention. J Am Dent Assoc. 2000; 131:887–899. [PubMed: 10916327]
25. Featherstone JD. The continuum of dental caries - Evidence for a dynamic disease process. J Dent Res. 2004; 83:C39–C42. [PubMed: 15286120]
26. Deng DM, ten Cate JM. Demineralization of dentin by *Streptococcus mutans* biofilms grown in the constant depth film fermentor. Caries Res. 2004; 38:54–61. [PubMed: 14684978]
27. Totiam P, Gonzalez-Cabezas C, Fontana MR, Zero DT. A new *in vitro* model to study the relationship of gap size and secondary caries. Caries Res. 2007; 41:467–473. [PubMed: 17827964]
28. Svanberg M, Mjör IA, Ørstavik D. Mutans streptococci in plaque from margins of amalgam, composite, and glass-ionomer restorations. J Dent Res. 1990; 69:861–864. [PubMed: 2109000]
29. Imazato S, Torii M, Tsuchitani Y, McCabe JF, Russell RRB. Incorporation of bacterial inhibitor into resin composite. J Dent Res. 1994; 73:1437–1443. [PubMed: 8083440]
30. Sousa RP, Zanin IC, Lima JP, Vasconcelos SM, Melo MA, Beltrao HC, et al. *In situ* effects of restorative materials on dental biofilm and enamel demineralization. J Dent. 2009; 37:44–51. [PubMed: 19026481]
31. Thome T, Mayer MPA, Imazato S, Geraldo-Martins VR, Marques MM. *In vitro* analysis of inhibitory effects of the antibacterial monomer MDPB-containing restorations on the progression of secondary root caries. J Dent. 2009; 37:705–711. [PubMed: 19540033]
32. Antonucci JM, Zeiger DN, Tang K, Lin-Gibson S, Fowler BO, Lin NJ. [0]Synthesis and characterization of dimethacrylates containing quaternary ammonium functionalities for dental applications. Dent Mater. 2011 in press.
33. Patel MP, Cruchley AT, Coleman DC, Swai H, Braden M, Williams DM. A polymeric system for the intra-oral delivery of an anti-fungal agent. Biomaterials. 2001; 22:2319–2324. [PubMed: 11511028]
34. Leung D, Spratt DA, Pratten J, Gulabivala K, Mordan NJ, Young AM. Chlorhexidine-releasing methacrylate dental composite materials. Biomaterials. 2005; 26:7145–7153. [PubMed: 15955557]
35. Anusavice KJ, Zhang NZ, Shen C. Controlled release of chlorhexidine from UDMA-TEGDMA resin. J Dent Res. 2006; 85:950–954. [PubMed: 16998139]
36. Palmer G, Jones FH, Billington RW, Pearson GJ. Chlorhexidine release from an experimental glass ionomer cement. Biomaterials. 2004; 25:5423–5431. [PubMed: 15130727]

37. Takahashi Y, Imazato S, Kaneshiro A, Ebisu S, Frenchen JE, Tay FR. Antibacterial effects and physical properties of glass-ionomer cements containing chlorhexidine for the ART approach. Dent Mater. 2006; 22:647–652. [PubMed: 16226806]
38. Skrtic D, Antonucci JM, Eanes ED, Eichmiller FC, Schumacher GE. Physiological evaluation of bioactive polymeric composites based on hybrid amorphous calcium phosphates. J Biomed Mater Res B. 2000; 53:381–391.
39. Dickens SH, Flaim GM, Takagi S. Mechanical properties and biochemical activity of remineralizing resin-based Ca-PO_4 cements. Dent Mater. 2003; 19:558–566. [PubMed: 12837405]
40. Langhorst SE, O'Donnell JNR, Skrtic D. *In vitro* remineralization of enamel by polymeric amorphous calcium phosphate composite: Quantitative microradiographic study. Dent Mater. 2009; 25:884–891. [PubMed: 19215975]
41. Xu HHK, Sun L, Weir MD, Antonucci JM, Takagi S, Chow LC. Nano dicalcium phosphate anhydrous-whisker composites with high strength and Ca and PO_4 release. J Dent Res. 2006; 85:722–727. [PubMed: 16861289]
42. Xu HHK, Weir MD, Sun L, Moreau JL, Takagi S, Chow LC, et al. Strong nanocomposites with Ca, PO_4 and F release for caries inhibition. J Dent Res. 2010; 89:19–28. [PubMed: 19948941]
43. Xu HHK, Moreau JL, Sun L, Chow LC. Strength and fluoride release characteristics of a calcium fluoride based dental nanocomposite. Biomaterials. 2008; 29:4261–4267. [PubMed: 18708252]
44. Xu HHK, Moreau JL, Sun L, Chow LC. Novel CaF_2 nanocomposite with high strength and F ion release. J Dent Res. 2010; 89:739–745. [PubMed: 20439933]
45. Xu HHK, Moreau JL, Sun L, Chow LC. Nanocomposite containing amorphous calcium phosphate nanoparticles for caries inhibition. Dent Mater. 2011; 27:762–769. [PubMed: 21514655]
46. Chow LC, Sun L, Hockey B. Properties of nanostructured hydroxyapatite prepared by a spray drying technique. J Res NIST. 2004; 109:543–551.
47. Sun L, Chow LC. Preparation and properties of nano-sized calcium fluoride for dental applications. Dent Mater. 2008; 24:111–116. [PubMed: 17481724]
48. Moreau JL, Sun L, Chow LC, Xu HHK. Mechanical and acid neutralizing properties and inhibition of bacterial growth of amorphous calcium phosphate dental nanocomposite. J Biomed Mater Res Part B. 2011; 98:80–88.
49. Lee Y, Lu H, Oguri M, Powers JM. Changes in gloss after simulated generalized wear of composite resins. J Prosthet Dent. 2005; 94:370–376. [PubMed: 16198175]
50. Exterkate RA, Crielaard W, Ten Cate JM. Different response to amine fluoride by *Streptococcus mutans* and polymicrobial biofilms in a novel high-throughput active attachment model. Caries Res. 2010; 44:372–379. [PubMed: 20668379]
51. van Loveren C, Buijs JF, ten Cate JM. The effect of triclosan toothpaste on enamel demineralization in a bacterial demineralization model. J Antimicrob Chemo. 2000; 45:153–158.
52. Kraigsley AM, Lin-Gibson S, Lin NJ. Effects of polymer degree of conversion on oral biofilm metabolic activity and biomass. J Dent Res. 2011 (in review).
53. Deng DM, van Loveren C, ten Cate JM. Caries-preventive agents induce remineralization of dentin in a biofilm model. Caries Res. 2005; 39:216–223. [PubMed: 15914984]
54. Stoodley P, Wefel J, Gieseke A, deBeer D, von Ohle C. Biofilm plaque and hydrodynamic effects on mass transfer, fluoride delivery and caries. J Am Dent Assoc. 2008; 139:1182–1190. [PubMed: 18762628]
55. Dawes C. What is the critical pH and why does a tooth dissolve in acid? J Can Dent Assoc. 2003; 69:722–724. [PubMed: 14653937]
56. Burne RA. Oral *Streptococci* … Products of their environment. J Dent Res. 1998; 77:445–452. [PubMed: 9496917]

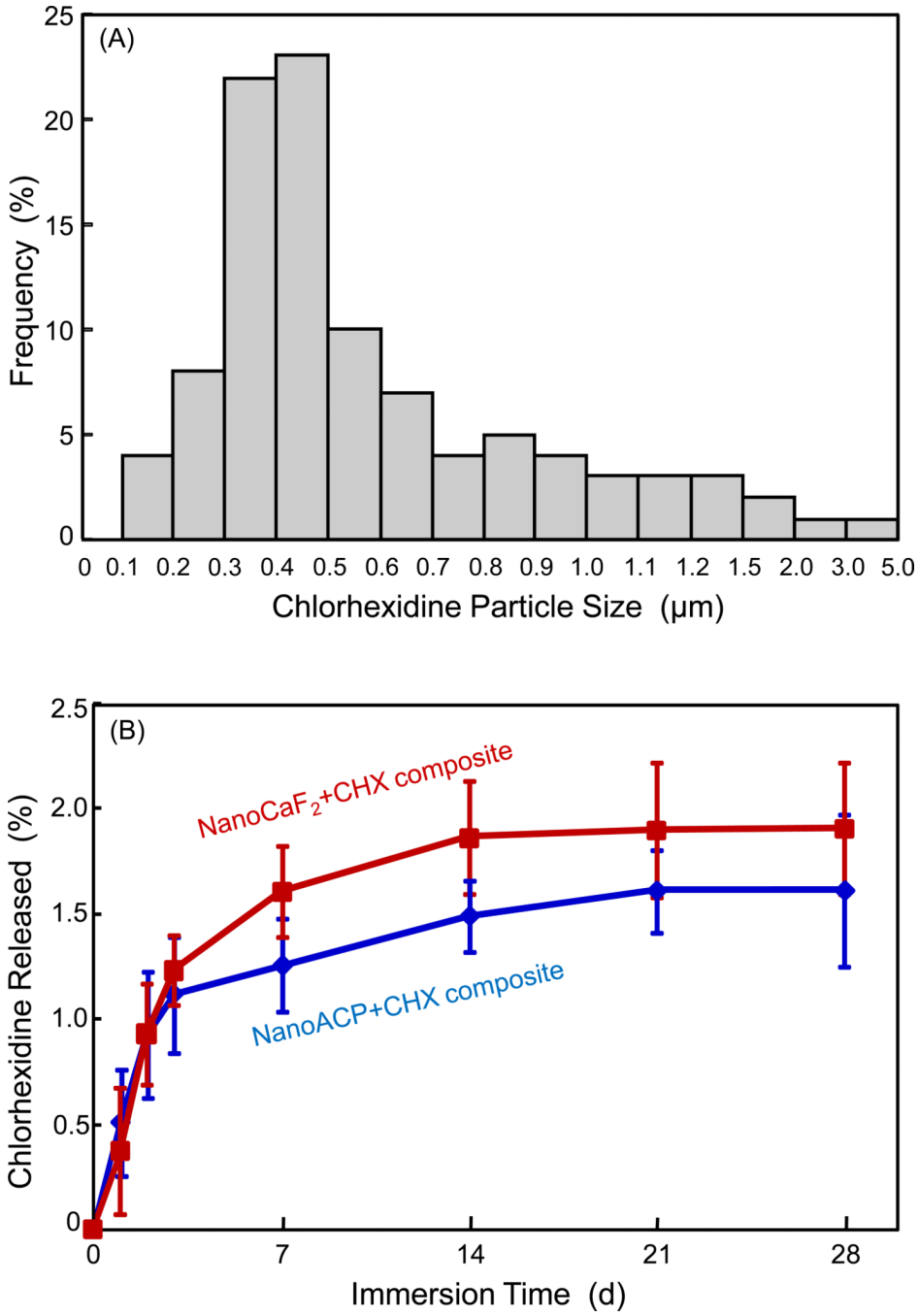

Figure 1.
(A) CHX particle size distribution, based on the measurement via SEM of 100 random particles. (B) CHX release from ACP and CaF_2 nanocomposites. Each value is the mean of three measurements with the error bar showing one standard deviation (mean ± sd; n = 3), with specimens immersed in a physiological solution at pH 7 from 1 d to 28 d.

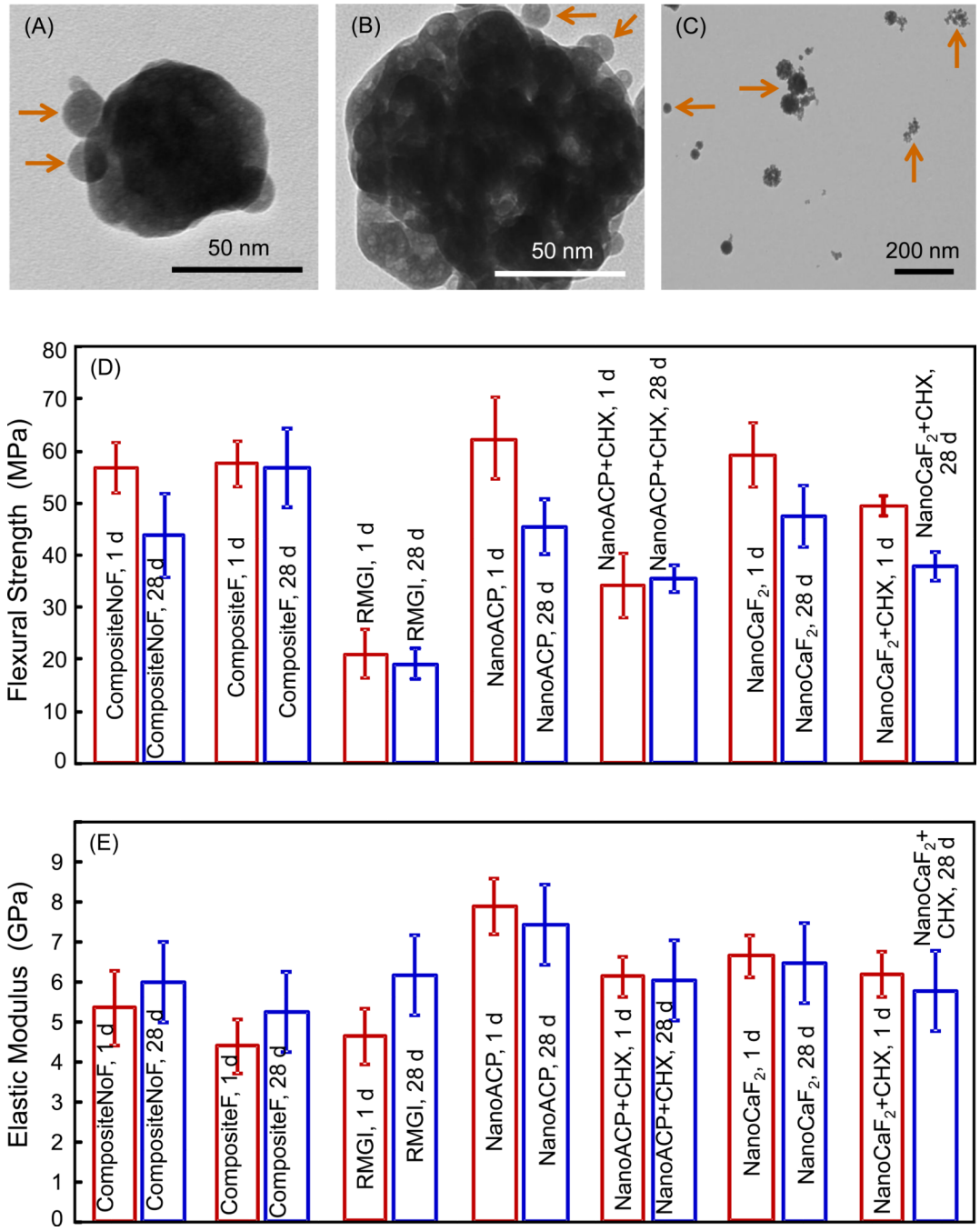

Figure 2.

TEM micrographs of the spray-dried nanoparticles as well as the composite mechanical properties. (A) Small ACP nanoparticles, (B) ACP cluster, (C) CaF_2 nanoparticles, (D) flexural strength, and (E) elastic modulus, after 1 d and 28 d of immersion. Each value is mean ± sd; n = 6. CompositeF is Heliomolar. CompositeNoF is Renamel. RMGI is Vitremer. NanoACP composite and $NanoCaF_2$ composite had no CHX. NanoACP+CHX and $NanoCaF_2$+CHX contained 10% CHX particles by mass.

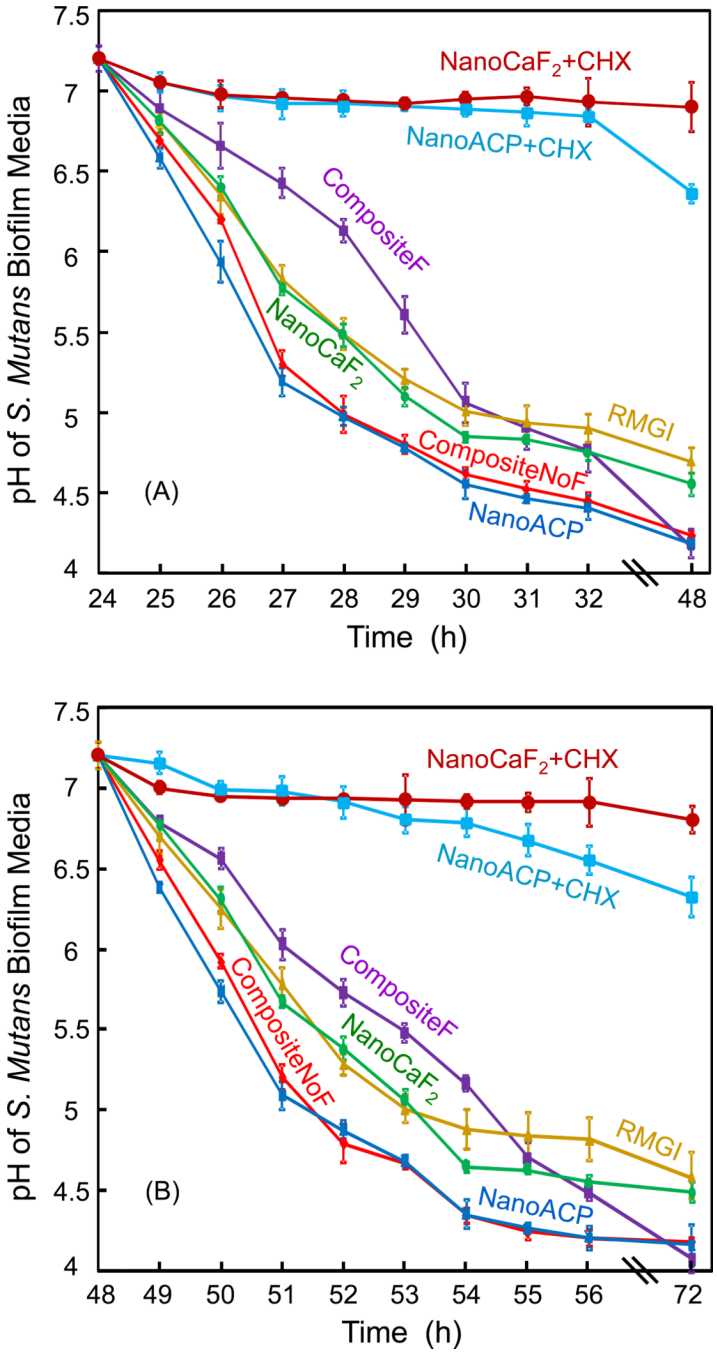

Figure 3.

The pH of the culture medium with biofilm on the composite disk. Each value is mean ± sd; n = 6. During the first 24 h after inoculation, an initial biofilm was established on the composite disk. At 24 h, the disk was transferred to a new well with new medium, and the pH measurement was started. The plot in (A) shows the pH from 24 h to 48 h. At 48 h, a new culture medium was used (because the medium was changed daily), and the pH is plotted in (B) from 48 h to 72 h. The initial pH was 7.2 for each new medium.

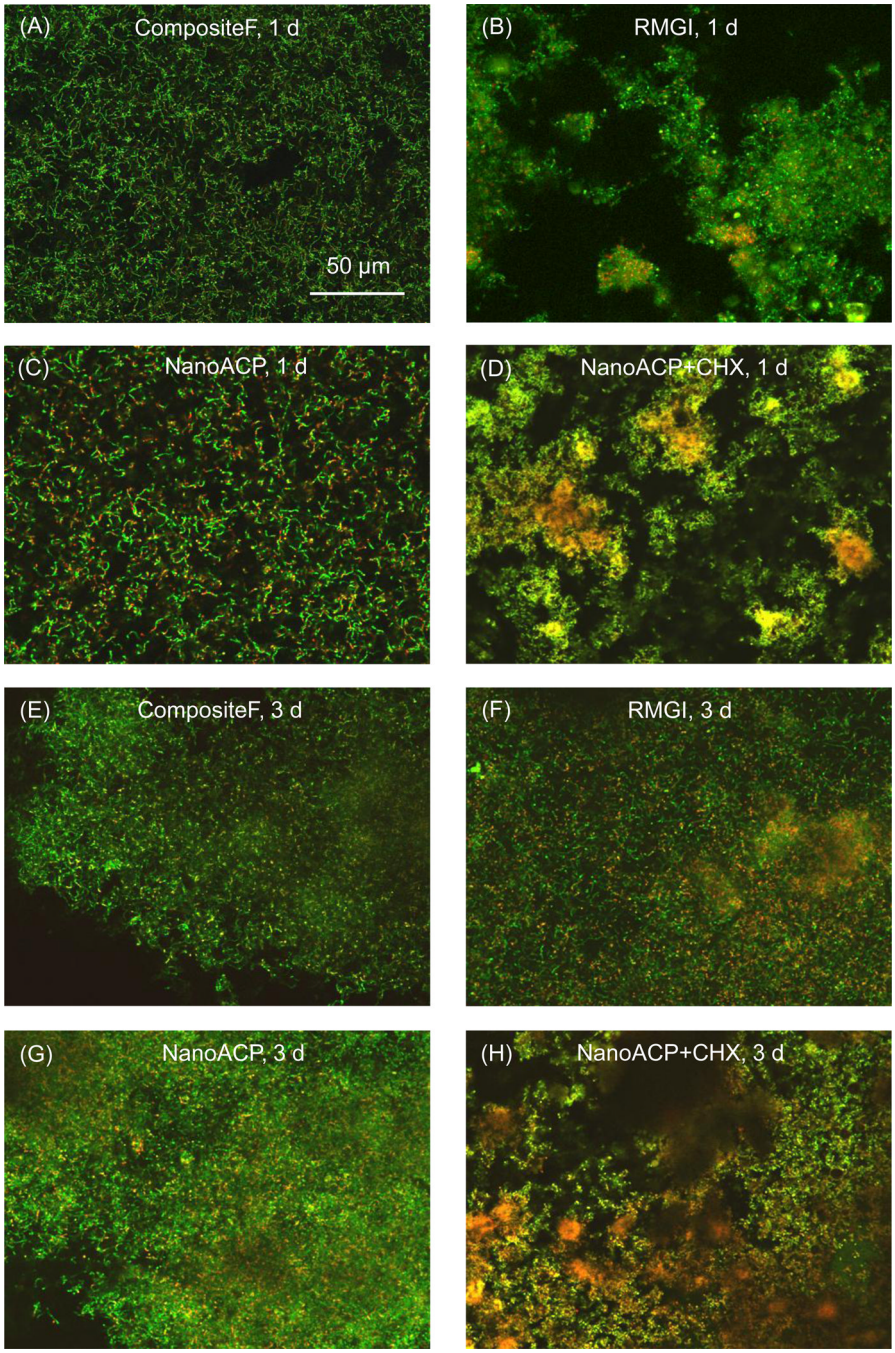

Figure 4.

Representative live/dead images: Early biofilms (1 d) are shown for (A) CompositeF, (B) RMGI, (C) NanoACP, and (D) NanoACP+CHX. Mature biofilms (3 d) are shown for the same materials in (E) to (H). Live bacteria appear green. Membrane-compromised bacteria appear red, and, when mingled with live bacteria, appear yellow/orange. At 1 d, bacteria were predominantly alive in (A) to (C), with some cell death in (B). (D) NanoACP+CHX had increased dead bacteria relative to (A) to (C). At 3 d, live bacteria formed mature biofilms in (E) to (G) with slightly increased death in (F). (H) NanoACP+CHX had significant amounts of dead bacteria. Images of CompositeNoF and NanoCaF$_2$, which had qualitatively similar features to the other materials without CHX, were omitted to save

space. Likewise, images for NanoCaF$_2$+CHX were not shown, as their biofilms had similar features to biofilms on the NanoACP+CHX.

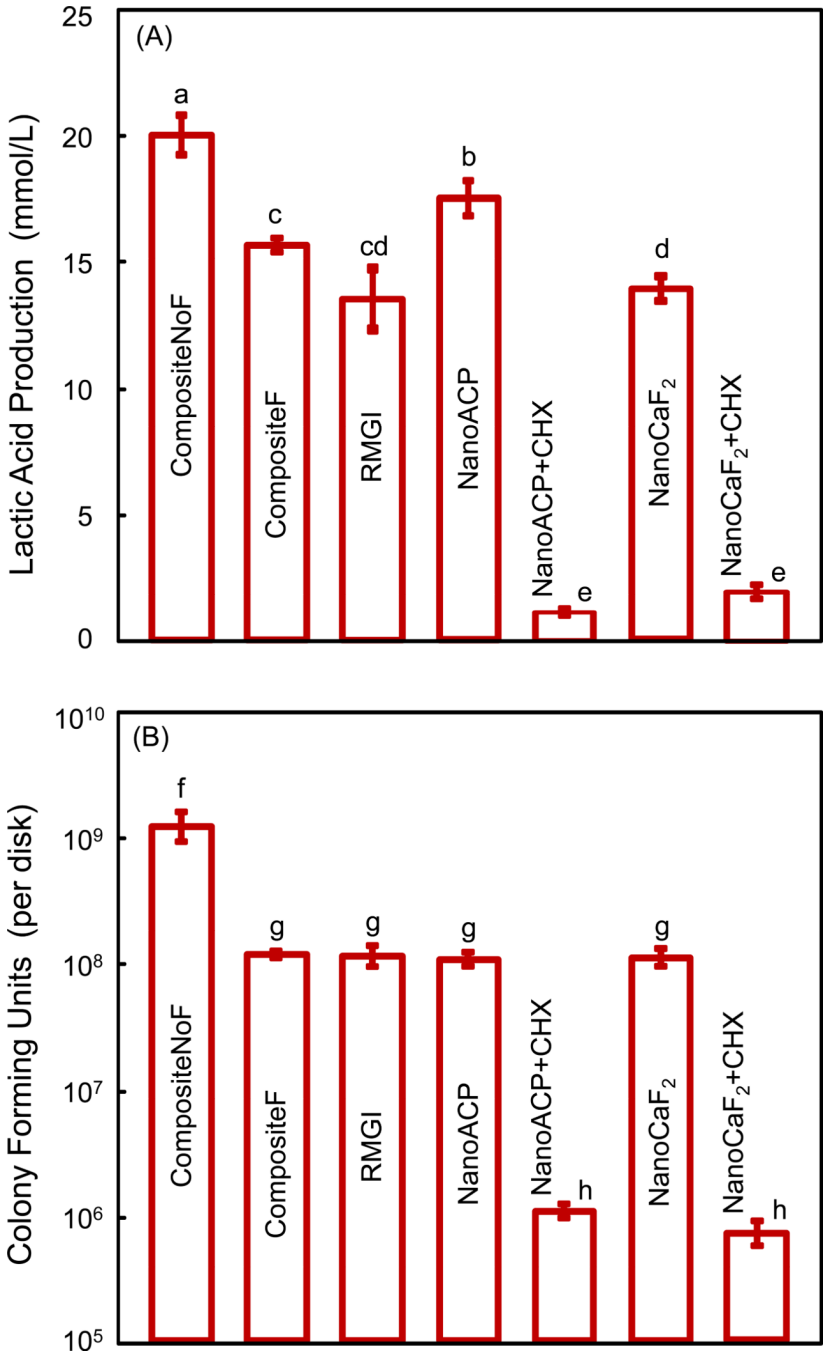

Figure 5.

Quantitative response of *S. mutans* biofilms on the composite disks: (A) Lactic acid production, and (B) bacteria colony-forming units (CFU) on the disks at 3 d. In each plot, dissimilar letters indicate values (mean ± sd; n = 6) that are different from each other ($p < 0.05$). Values with the same letters are not significantly different ($p > 0.1$).

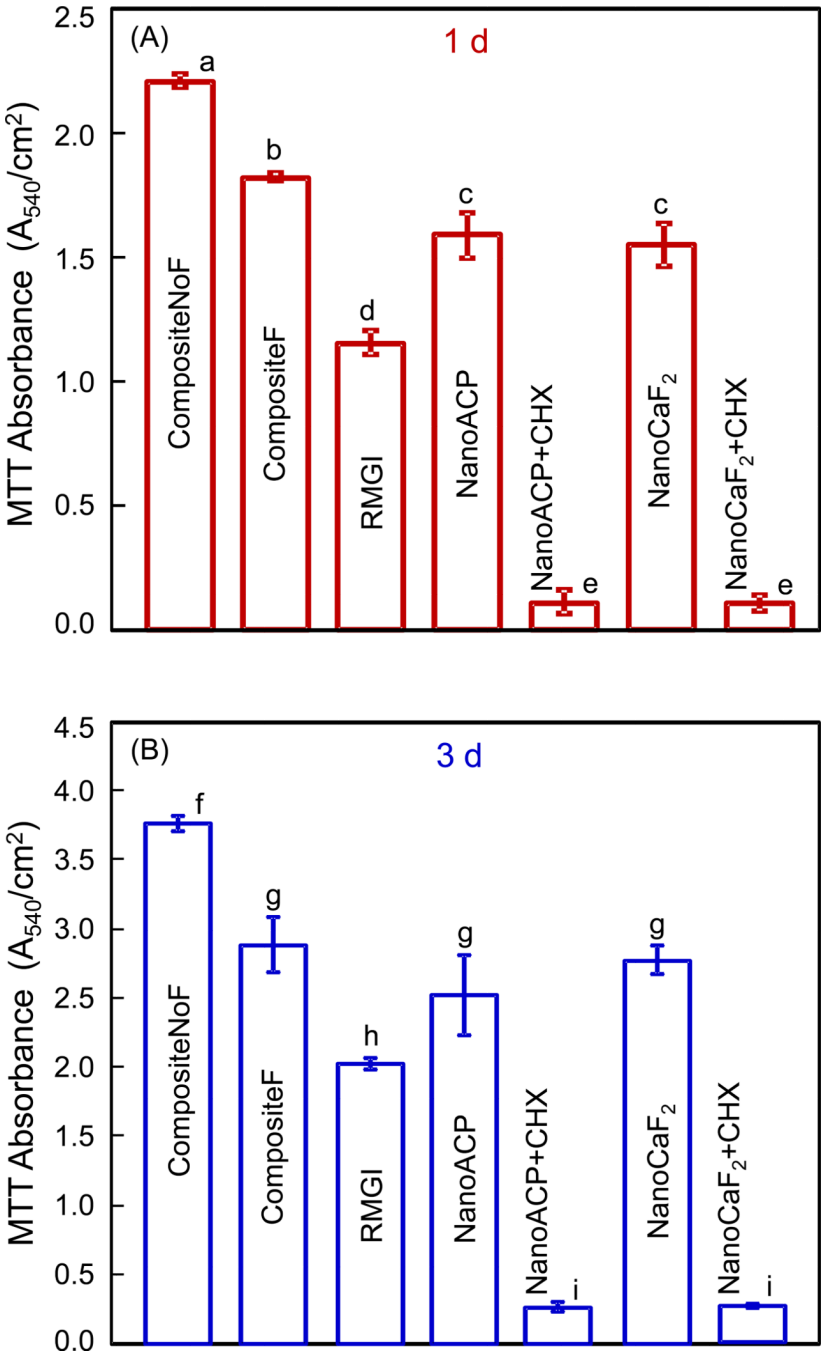

Figure 6.

Results of the MTT metabolic activity assay for *S. mutans* on composite disks at: (A) 1 d, and (B) 3 d. A higher absorbance indicates an overall higher metabolically active biofilm on the composite disk that metabolized the MTT tetrazole. In each plot, values (mean ± sd; n = 6) with dissimilar letters are significantly different from each other ($p < 0.05$). Values with the same letters are not significantly different ($p > 0.1$).